Biophysical properties of *Saccharomyces cerevisiae* and their relation to HOG pathway activation

Supporting Information

Jörg Schaber[a,g,1], Miquel Àngel Adrover[b,2], Emma Eriksson[c,h,2], Serge Pelet[d,2], Elzbieta Petelenz-Kurdziel[e,2], Dagmara Klein[e,f], Francesc Posas[b], Mattias Goksör[c], Mathias Peter[d], Stefan Hohmann[e], Edda Klipp[a,1]

[a] Theoretical Biophysics, Humboldt University, Invaliden Str. 42, 10115 Berlin, Germany

[b] Cell Signaling Unit, Departament de Ciències Experimentals i de la Salut, Universitat Pompeu Fabra (UPF), E-08003 Barcelona, Spain

[c] Department of Physics, University of Gothenburg, SE-412 96 Gothenburg, Sweden

[d] Institute of Biochemistry, ETH, Zurich, Switzerland

[e] Department of Cell and Molecular Biology/Microbiology, University of Gothenburg, Box 462, SE-405 30 Göteborg, Sweden

[f] present address: Clinical R&D Laboratory - Oxoid, Microbiology - Basingstoke, Thermo Fisher Scientific, UK

[g] Institute for Experimental Internal Medicine, Medical Faculty, Otto-von-Guericke University, Leipziger Str. 44, 39120 Magdeburg, Germany

[h] present address: SP Technical Research Institute of Sweden, Brinellgatan 4, Box 857, SE-501 15 Borås, Sweden

[1] To whom correspondence should be addressed:

Jörg Schaber
Institute of Experimental Internal Medicine
Medical Faculty
Otto von Guericke University
Leipziger Str. 44, 39120 Magdeburg, Germany
Phone: +49 391 67 14453
Fax: +49 391 67 13312
Email: schaber@med.ovgu.de

Edda Klipp
Theoretical Biophysics
Humboldt University
Invalidenstr. 42
10115 Berlin, Germany
Phone: +49 30 2093 9040
Fax: +49 30 2093 8813
Email: edda.klipp@rz.hu-berlin.de

[2] M.A.A., E.E, S.P. E.P.K. contributed equally.

Modelling framework

Units and descriptions of variables and parameters that are also used in the main text are listed in Table 1 of the main text.

Volume model

The linear elastic theory states that the change in turgor pressure *P* is proportional to a relative change in membrane enclosed cell volume V_m, i.e.,

$$dP = \varepsilon \frac{dV_m}{V_m},$$

where ε is a proportionality factor, called volumetric elastic modulus or bulk modulus. The factor ε in Eqn.1 reflects properties of the cell wall and may change according to a change a cell wall composition. In this study, we consider a population of cells within a short time interval and we assume that the average cell wall composition within this time frame does not alter significantly. Therefore, within the scope of this study, it seems reasonable to treat ε as a constant. Even though ε is usually assumed to reflect properties of the cell wall, it is important to note that V_m in Eqn. 1 represents the cytoplasmic volume enclosed by the plasma membrane. It is within V_m where osmotic and hydrostatic pressures are defined. V_m comprises the osmotically active volume V_{os} and the solid volume V_b of the cytoplasm, i.e. $V_m = V_{os} + V_b$. However, the commonly measured volume is that enclosed by the cell wall, which here we refer to as the apparent volume V_{ap}. It is generally assumed that $V_{ap} = V_m$. This assumption may be unproblematic in the case of turgid cells where the membrane is closely attached to the cell wall. However, plasmolysis may occur upon sudden shrinkage, such that the membrane detaches from the cell wall. Indeed, following hyperosmotic shock, the membrane exhibits invaginations and projections into the cytoplasm, indicating that it detaches from the cell wall [S1-4]. In this situation, changes in V_m might not be observable because the cell wall no longer follows the membrane changes. Thus, it might be more realistic to assume that $V_{ap} = V_m + V_{pl}$, where V_{pl} is a measure for the periplasmic volume between membrane and cell wall.

We assume that the change in osmotically active volume V_{os} is merely a function of water flow across the cell membrane, which in turn is a function of differences in chemical water potentials between inside and outside the cell, conveniently expressed as pressures:

$$\frac{dV_{os}(t)}{dt} = -L_p A\left(\Delta P + \frac{RT}{\overline{V}_w}\ln\frac{a_w^i}{a_w^e} - \Delta\tau\right), \qquad \text{Eqn. S1}$$

where L_p is the hydraulic conductivity [μm MPa^{-1} s^{-1}], A [μm^2] is the surface of V_{os}, R is the gas constant [J K^{-1} mol^{-1}], T is the temperature [K], $\overline{V}_w$ is the partial molar volume of water, $\Delta P = P^i - P^e$ is the hydrostatic pressure difference, i.e. the turgor [MPa], and $\Delta\tau = \tau^i - \tau^e$ is the matrix potential difference between inside and outside of the cell, respectively, denoted by superscripts *i* and *e*, and a_w is the water activity. We define P as the pressure above atmospheric pressure and assume that the outside of the cell is under atmospheric pressure, thus $\Delta P = P^i = P$. We also assume that τ^e is negligible. The internal matrix potential τ^i arises from electrostatic interactions between liquid and colloidal interfaces of the intracellular liquid, such as protein surfaces for instance, that are generally attractive ($\tau > 0$). Water that is partly bound to colloids or proteins is not as freely available as unbound water in solution and larger forces must be applied to mobilize this water. This lowers the chemical potential of the total intracellular water by an amount that is termed the matrix potential [S5]. It can also be imagined that the cytoskeleton counteracts cell shrinkage by mechanical forces such that the cell has an inherent tendency to re-swell, like a sponge. This effect would also lower the total intracellular water potential. We summarize all effects that lower the water potential under the term internal matrix potential τ^i. However, it is unclear, whether the intracellular fluid can be subjected to such a macroscopic thermodynamic description at all. Therefore splitting the chemical water potential into hydrostatic, osmotic and matrix potential is somewhat arbitrary. For example, the threshold in particle size between an osmotic and a matrix contributor remains elusive [S5,S6]. In this work, we assume that τ plays a role only when cell volume becomes small (see below). In particular, we consider the initial matrix potential as negligible, i.e. $\tau_0 = 0$.

Assuming that the concentrations of osmotically active solutes are sufficiently small [S5,S7-S9], Eqn.1 can be formulated as

$$\frac{dV_{os}(t)}{dt} = -L_p A\left(P(V_m) + \alpha_{PC} RT\left(c^e(t) - c^i(t)\right) - \tau(V_m)\right), \qquad \text{Eqn. S2}$$

where, for the lack of other quantitative descriptions, we consider both turgor *P* and the matrix potential τ as a function of V_m (Eqn. 3). c^e and c^i [Osm/L] denote external and internal osmolarities, respectively and α_{PC} is a dimensionless conversion factor relating pressure units to osmolarity.

When both water and solutes are transported through the membrane the so-called reflection coefficient σ should be considered [S7,S8]. However, when water and solutes are transported by different channels, which can be assumed to be the case in yeast with glycerol as the permeable solute, then

$$\sigma = 1 - \frac{k_s \overline{V}}{RTL_p} \quad ,$$

where $\overline{V}$ is the partial molar volume of the solute, k_s [μm s^{-1}] is the membrane solute permeability. In the case of glycerol ($\overline{V} \approx 0.071 \cdot 10^{-3}$ m^3/mol) as the only solute σ approximates unity at room temperature. Thus, the reflection coefficient is not further considered here [S9,S10].

When yeast cells are subjected to a hyperosmotic shock, i.e. the external osmolarity c^e rises quickly, they rapidly shrink to a certain minimal volume $V_m^{\min}$ due to the passive balancing of internal and external water potentials. Subsequently, they gradually re-swell due to a further increase in the internal osmolarity c^i, achieved by both producing and retaining glycerol as an osmotically active and permeable compound [S11-S14].

Since $V_m^{\min}$ is attained very quickly, usually within a time range from seconds up to two minutes [S11,S15,S16], we can presume that osmotically active substances neither accumulate inside nor leave the cell and, thus, c^i increases only due to the volume decrease mediated by water flow. Moreover, in order to compare theoretical $V_m^{\min}$ with experimental data, we have to take into account that $V_{os} = V_{ap} - V_b - V_{pl}$.

Therefore, when $V_m^{\min}$ is reached, by definition,

$$0 = P_{V_m^{\min}} - \tau_{V_m^{\min}} + \alpha_{PC} RT \left(c^e - c_0^i \frac{V_{ap}^0 - V_b - V_{pl}}{V_{ap}^{\min} - V_b - V_{pl}} \right), \qquad \text{Eqn. S3}$$

where $P_{V_m^{\min}}$ and $\tau_{V_m^{\min}}$ are the turgor pressure and the matrix potential at $V_m^{\min}$, respectively, and V_{ap}^0 is the initial apparent cell volume. We also assume that the intracellular osmotically active solutes reside in the osmotically active volume V_{os} and not in the solid volume V_b. Osmotically active solutes are usually considered to be small molecules, like, e.g. glycerol or NaCl, and therefore this assumption seems justified.

Assuming that Eqn. S2 is initially at steady state, i.e. $\frac{dV_{os}}{dt} = 0$, and $\tau_0 = 0$, then we can estimate the initial internal concentration c_0^i as a function of the initial turgor P_0 and the initial external osmolarity c_0^e as

$$c_0^i = c_0^e + \frac{P_0}{\alpha_{PC} RT}. \qquad \text{Eqn. S4}$$

Given Eqn. S4, we can now calculate $V_{ap}^{\min}$ from Eqn. S3 as a function of c_0^e, P_0, $V_m^{\min}$, $P_{V_m^{\min}}$, $\tau_{V_m^{\min}}$ and the stress $c_{stress}^e = c^e - c_0^e$ we apply:

$$V_{ap}^{\min} = V_b + V_{pl} + \frac{c_0^i \left(V_{ap}^0 - V_b - V_{pl} \right)}{\frac{P_{V_m^{\min}} - \tau_{V_m^{\min}}}{\alpha_{PC} RT} + c_{stress}^e + c_0^e}. \qquad \text{Eqn. S5}$$

When turgor and matrix potential equal zero, Eqn. S5 simplifies to van't Hoff's equation, where volume is a reciprocal function of the total external osmolarity

$$V_{ap}^{\min} = V_b + V_{pl} + \frac{c_0^i \left(V_{ap}^0 - V_b - V_{pl} \right)}{c_{stress}^e + c_0^e}. \qquad \text{Eqn. S6}$$

Turgor and matrix potential models

From Eqn. 1 of the main text we can deduce an expression for *P* by integration:

$$\int_{V_m^i}^{V_m} dP(V) = \int_{V_m^i}^{V_m} \varepsilon \frac{1}{V} dV$$

$$\Leftrightarrow P(V_m) - P(V_m^i) = \varepsilon \ln\left(\frac{V_m}{V_m^i}\right)$$

Defining $V_m^i = V_m(P=0) = V_m^{P=0}$ as the volume, where turgor becomes zero, i.e. $P(V_m^{P=0}) = 0$, and further assuming that $V_{pl} = 0$ for $V_m \geq V_m^{P=0}$ we arrive at an expression for turgor as a function of the apparent volume,

$$P(V_{ap}, V_m^{P=0}, \varepsilon) = \varepsilon \ln\left(\frac{V_{ap}}{V_m^{P=0}}\right) \text{ for } V_m \geq V_m^{P=0} \text{ and } V_{ap} = V_m . \qquad \text{Eqn. S7}$$

Several possibilities may happen for $V_{ap} < V_m^{P=0}$. Most models assume that below $V_m^{P=0}$, turgor is negligible [S11,S12,S14,S17]. To this model we will refer as the one-sided model (Figure 2 in the main text). One could also assume that the cell actually resists further compression below $V_m^{P=0}$ by the cytoskeleton, for instance, like a sponge. This means that, in addition to the water flow, a force must be applied to further compress the cells. This could be modelled by a negative turgor also according to the linear elastic model. Moreover, as mentioned above, we consider τ only when V_m becomes small. In this situation, a fraction of intracellular water may be bound to colloidal surfaces, thus, electrostatic effects might become important. Lacking other quantitative descriptions, we model τ similar to *P*, such that below a certain volume we combine matrix and other effects leading to a decrease in water potential, i.e $P_{V_{ap}^{\min}} = P_{V_m^{\min}} - \tau_{V_m^{\min}}$, leading to

$$P_{V_{ap}^{\min}}(V_{ap}^{\min}, V_{pl}, V_m^{P=0}, V_m^{\tau}, \varepsilon, \varepsilon_{\tau}) = \begin{cases} \varepsilon \ln\left(\dfrac{V_{ap}^{\min}}{V_m^{P=0}}\right) & \text{for } V_{ap}^{\min} \geq V_m^{P=0} \\ 0 & \text{for } V_m^{\tau} \leq V_{ap}^{\min} - V_{pl} < V_m^{P=0} \\ \varepsilon_{\tau} \ln\left(\dfrac{V_{ap}^{\min} - V_{pl}}{V_m^{\tau}}\right) & \text{for } V_{ap}^{\min} - V_{pl} < V_m^{\tau} \end{cases} \qquad \text{Eqn. S8}$$

where ε_{τ} is a proportionality factor [MPa] similar to ε. Eqn. 8 we will call the two-sided model in the following (see Figure 2 main text).

Thus, Eqn. S5 becomes

$$V_{ap}^{\min} = V_b + V_{pl} + \frac{c_0^i\left(V_{ap}^0 - V_b - V_{pl}\right)}{\frac{P_{V_{ap}^{\min}}(V_{ap}^{\min}, V_{pl}, V_m^{P=0}, V_m^{\tau}, \varepsilon, \varepsilon_\tau)}{\alpha_{PC} RT} + c_{stress}^e + c_0^e} \qquad \text{Eqn. S9}$$

There exist several possibilities how to treat V_{pl}. First, we can assume that always $V_{pl} = 0$. A second option is to anticipate that the membrane starts detaching from the cell wall upon a certain c_{pl}^e from where the cell wall no longer shrinks and therefore a constant $V_{ap}^{pl} = V_b + \frac{c_0^i\left(V_{ap}^0 - V_b - V_{pl}\right)}{\frac{P_{V_{ap}^{\min}}}{\alpha_{PC} RT} + c_{pl}^e + c_0^e}$ is attained. This is the option depicted in Figure 1 of the main text. Thus, rearranging Eqn. S9, V_{pl} can be calculated in this case by

$$V_{pl} = \frac{\left(V_{ap}^{pl} - V_b\right)\left(\frac{P_{V_{ap}^{\min}}}{\alpha_{PC} RT} + c_{stress}^e + c_0^e\right) - c_0^i\left(V_{ap}^0 - V_b\right)}{\frac{P_{V_{ap}^{\min}}}{\alpha_{PC} RT} + c_{stress}^e + c_0^e - c_0^i} \quad \text{for} \quad c_{stress}^e > c_{pl}^e, \qquad \text{Eqn. S10}$$

A third hypothesis which we tested is that the cell membrane detaches from the cell wall as soon as $V_{ap} < V_{ap}^{pl}$ and that $dV_{pl} = -\varepsilon_{pl} dV_{ap} / V_{ap}$, which leads to

$$V_{pl} = \varepsilon_{pl} \ln\left(\frac{V_{ap}^{pl}}{V_{ap}}\right). \qquad \text{Eqn. S11}$$

Thus, the minimal volume attained after an osmotic shock is an implicit function of V_{ap}, depending on three to seven parameters P_0, ε, V_b, ε_τ, V_{ap}^{τ}, V_{ap}^{pl} and ε_{pl} according to the employed turgor and volume models, and the measureable final external osmolarity after stress $c^e = c_{stress}^e + c_0^e$ and initial apparent volume V_{ap}^0, where P_0 is needed to calculate c_0^i by Eqn. S4 and $V_m^{P=0} = V_{ap}^0 e^{-\frac{P_0}{\varepsilon}}$ by Eqn. S7.

In Table S1 we summarize the tested models, with their number of parameters and assumptions:

Table S1: Minimal volume models based on Eqn. S5.

#	Model	Turgor and τ	V_{pl}	#p	Estimated parameters
1	van't Hoff	Eqn. S6	$V_{pl}=0$	1	V_b
2	One-sided	Eqn. S7	$V_{pl}=0$	3	P_0, ε, V_b
3	Two-sided	Eqn. S8	$V_{pl}=0$	5	P_0, ε, V_b, ε_τ, V_{ap}^{τ}
4	Constant $V_{ap}^{\min}$	Eqn. S7	Eqn. S10	4	P_0, ε, V_b, c_{pl}^{e}
5	Two-sided constant $V_{ap}^{\min}$	Eqn. S8	Eqn. S10	6	P_0, ε, V_b, ε_τ, V_{ap}^{τ}, V_{ap}^{pl}
6	Log V_{pl}	Eqn. S7	Eqn. S11	6	P_0, ε, V_b, ε_τ, V_{ap}^{pl}, ε_{pl}
7	Two-sided Log V_{pl}	Eqn. S8	Eqn. S11	7	P_0, ε, V_b, ε_τ, V_{ap}^{τ}, V_{ap}^{pl}, ε_{pl}

Alternatively, V_{ap}^{τ} and V_{ap}^{pl} can be set to $V_m^{P=0}$ thereby deceasing the number of parameters to be estimated.

Proof of a unique solution of Eqn. S9 (Eqn. 2 in the main text)

Rearranging Eqn. S9 we arrive at

$$P_{V_{ap}^{\min}}(V_{ap}^{\min},V_{pl},V_m^{P=0},V_m^{\tau},\varepsilon,\varepsilon_\tau)=\alpha_{PC}RT\left(\frac{c_0^i\left(V_{ap}^0-V_b-V_{pl}\right)}{V_{ap}^{\min}-V_b-V_{pl}}-(c_{stress}^e+c_0^e)\right)$$

For a given set of parameters $V_{pl},V_m^{P=0},V_m^{\tau},\varepsilon,\varepsilon_\tau$ and applied stress c_{stress}^e, the left hand side is a monotonically increasing function of $V_{ap}^{\min}$ (see Eqn. S8 and Figure 2 in the main text) and the right hand side is a monotonically decreasing function of $V_{ap}^{\min}$, with a singularity at V_b+V_{pl}. Therefore, in case there is a $V_{ap}^{\min}$, which satisfies the above equation between V_b+V_{pl} and V_{ap}^0, it must be unique.

Materials and Methods

In order to determine the parameters for selecting the most suitable model, we collected three independent data sets (Fig. 3, data set 1-3) and compared them with a data set (Fig. 3, data set 4) taken from literature [S11]. The cell volume was measured immediately before and directly after the hyper-osmotic stress, ensuring that we measured the minimal volume after osmotic shock. For our experiments we used NaCl as an osmoticum, whereas in the data set from literature yeast cells were subjected to a wide range of glycerol concentrations (refer to [S11] for details about the measurement). The data sets 1-4 are listed at the end of this section.

For reasons of a better comparison of the different data sets among each other, the information in Fig. 1 of the main text is displayed again with the osmotic shock in Osmolar [Osm/L] in Fig S1 and S2.

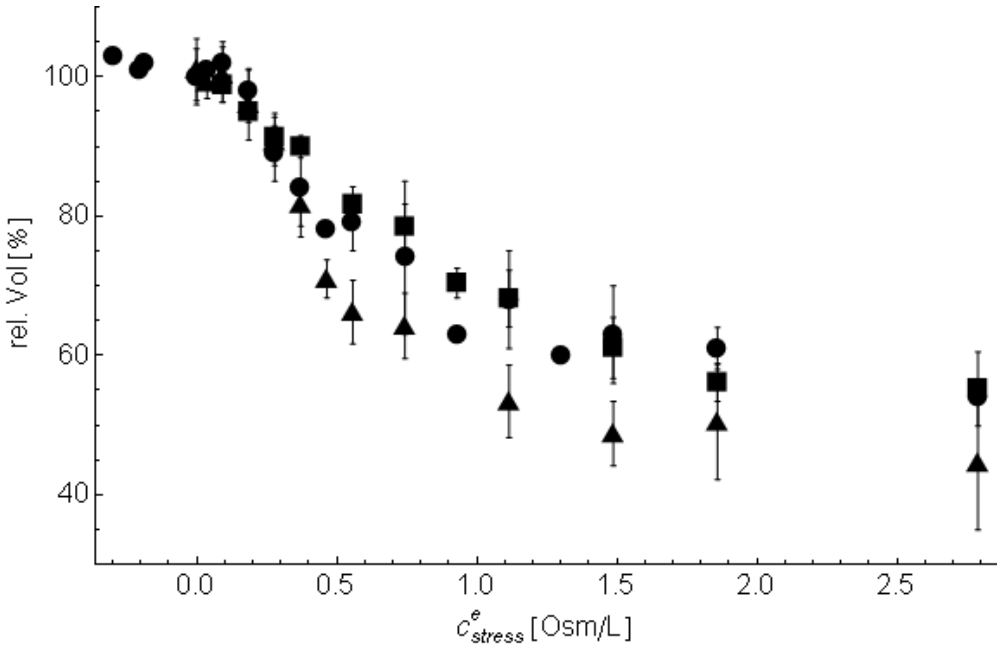

Figure S1: Minimal volume measurements of yeast cells subjected to an osmotic shock using NaCl [Osm/L]. **Circles**: data set no. 1 (mean and standard deviation of 3-5 population medians, if available). **Squares**: data set no. 2 (means and standard deviations of 11-24 cells). **Triangles**: data set no. 3 (means and standard deviations of 30 to 130 cells). Negative values of c^e_{stress} indicate a hypo-osmotic shock.

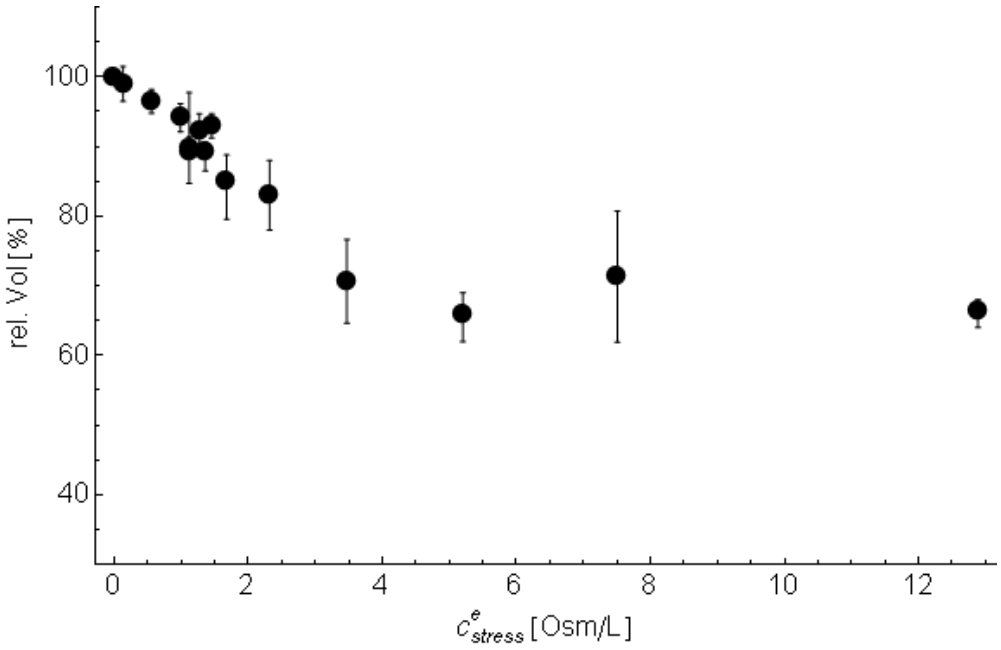

Figure S2: Minimal volume measurements of yeast cells subjected to an osmotic shock using glycerol [Osm/L] (mean and standard deviation). Data set no. 4, adapted and reproduced from [S11].

Coulter counter data (data set no. 1)

Wild type yeast cells (W303) were grown in YPD to saturation (OD_{660} = 4). A population of small G_1 synchronized cells was separated by centrifugal elutriation in YPD at 30ºC, re-suspended in fresh medium and grown at 30º C for one hour to approximately 40 fl of cell volume. Cells were stressed with 0.02 to 1.5 M NaCl or diluted into distilled water in order to apply hypo-osmotic shock from -0.05 to -0.2 Osmolar, assuming an initial osmotic pressure of the medium of 0.26 Osm/L, which was determined by freezing point depression. Samples were taken two minutes after stress was applied and fixed in 4% formaldehyde. Cell size distributions of at least 10000 cells were determined with a Beckman Z2 Coulter Counter. The minimal volume was determined as the mean of the medians for each measurements. Error bars (Fig. 6 in the main text) represent the standard deviation of the medians for at least three repetitions. The mean of the median, mean, standard deviation, skew and kurtosis of the distributions of absolute cell volumes of non-stressed cells was 39.3, 42.4, 18.2, 1.2, and 4.5 fl, respectively. Thus, the volume distributions of elutriated cells were close to a normal distribution.

Single cells bright field (data set no. 2)

Yeast cells (BY4741 Hog1-GFP) were cultured at 30°C on a gyratory shaker (220 rpm), in YNB medium (YNB complete, 2xCSM, 2% glucose) up to mid log phase (OD_{600}≈0.5-0.9) and introduced into the microfluidic channel system pre-treated with concanavalin A. The stress medium was prepared from YNB (YNB complete, 2xCSM, 2% glucose) and NaCl from a stock solution of 5 M (in water). The osmolarities (mOsm) of the stress solutions are shown in Table S2.

Table S2: Osmolarities of stress solutions for data set no. 2

NaCl concentration (M)	Osmolarity (mOsm)
0	267
0,05	346
0,1	436
0,15	535
0,2	630
0,3	824
0,4	1013
0,5	1174
0,6	1385
0,8	1793
1	2128
1,5	not measurable

The NaCl stress of single yeast cells was performed using a microfluidic system combined with optical tweezers [S18]. The microfluidic device had three inlet channels that were combined into a single wide channel. One channel was used for the NaCl containing medium (with appropriate concentration), one for pure YNB and one for the introduction of cells. The optical tweezers were used to position the cells on the bottom of the device, downstream of the junction where YNB and YNB+NaCl met. To allow the cells to attach to the surface, the microfluidic device was treated with a solution of concanavalin A for one hour before the experiment. During positioning, the salt flow was kept low, but at the start of the experiment the salt flow was increased and the two other flows turned off, thus providing a fast switch of environment around the cells. Images were acquired with a Leica DMI6000B inverted epi-fluorescence microscope equipped with a Hamamatsu C9100-12 EMCCD camera using a Leica, 100x NA1.3 microscope objective. Cell positioning, control of the microfluidic pumps and image acquisition (bright field) were controlled from OpenLab (Improvision). Images taken before the stress and after 90s of stress were segmented using CellID [S19,20]. The measurement of the area, "`a.tot.m1`", was found to best correspond to the apparent size of the yeast cells. This area was extrapolated to a volume assuming the cell to be a sphere, using Matlab. Finally, the relative volume (volume after stress divided by volume before stress) was calculated, and the mean and standard deviation were determined for each of the measured

concentrations. On average 18 cells were segmented correctly per concentration. Before stress the minor axis of the cells was measured to be 3.7µm ± 0.4µm.

Single cells fluorescence (data set no. 3)

Yeast cells (W303) with Hta2p-CFP, Hog1p-mCherry and cytoplasmic YFP were grown in SD medium and kept in log phase growth for more than 24 hours by several dilutions. Cells at OD_{600} 0.1 were further diluted 20 fold in SD-full, and briefly sonicated before 200µl of this cell culture solution were added to a well slide (Nunc, Lab-Tek 155411) previously coated with concanavalinA (0.5mg/ml). The cells were imaged on a Zeiss 200M microscope with a motorized XY stage and an incubation chamber set at 30°C. A 63x objective and appropriate fluorescence filter sets were used to record pictures of the cells in the RFP, CFP and YFP channels. Multiple positions in the well-slides were chosen and three images were recorded at each position before the stress. After the addition of 100µl of a three-fold concentrated NaCl solution in SD medium, time-lapse pictures were recorded with a time interval varying from 30 seconds to 5 minutes. The data acquired were automatically analysed with image analysis routines written in Matlab. Individual cells were tracked using a segmentation of the CFP images providing the nucleus of each cell. The cell area was obtained by segmentation of the YFP image (S Pelet, F. Rudolf and M.Peter *in preparation*). The volume was extrapolated from these area measurements assuming assuming a spherical shape. The volume change is calculated as following: $\Delta V = (V_{min} - V_{init})/ V_{init}$ where V_{init} is the initial volume calculated from the mean of the first three time points before the stress and V_{min} is the minimal volume of the cell reached after the osmotic stress. Median values and standard deviations of the volume change were calculated from 30 to 130 cells on average. Mean absolute cell volume of non-stressed cells was 56.5 fl with a standard deviation of ~19 fl for 870 cells.

Based on the nuclear and cell objects found by the segmentation routine, a third sub-nuclear region was defined with pixels contained in the cell object and within a distance of 5 pixels of the nucleus but not touching it. The Hog1p nuclear accumulation was measured by calculating the difference in intensity of the mean of the 20 highest intensity pixels between the nuclear and sub-nuclear object in the RFP channel. This analysis allowed to remove artefacts created by the cell shrinking which leads to an increased in nuclear fluorescence intensity upon osmotic shock independent of Hog1p activation.

Hog1 Western blots

The western blotting experiments were performed on the W303-1A strain (*MATa leu2-3/112 ura3-1 trp1-1 his3-11/15 ade2-1 can1-100 GAL SUC2 mal0*) [S21], cultured in YPD medium (Yeast Peptone D-glucose; 1% yeast extract (Bacto), 2% peptone (Bacto), 2% glucose). The cultures were grown until mid exponential phase (OD_{600}=0.7-1.0) and stressed with NaCl from a 5 M stock solution. Cell pellets obtained from 1 ml samples were frozen in liquid nitrogen at indicated time points. Proteins were extracted from the pellets by boiling for 10 min in extraction buffer (100mM Tris-HCl pH 6.8, 20% glycerol, 200mM DTT, 4% SDS, 10mM NaF, 0.1 mM Na_3V0_4 (sodium orthovanadate), protease inhibitor (Complete EDTA-free Protease Inhibitor Cocktail tablets, Roche), and 20mM mercapto-ethanol). The protein extracts were purified by centrifuging at 13000 rpm in 4^{o}C for 10 min. For each sample 20 μg of protein was electrophoresised on a 10% polyacrylamide gel (SDS-PAGE) and transferred to a nitrocellulose membrane (Hybond-ECL, Amersham). Membranes were blocked with 5% milk (Difco) in TBST and incubated with antibodies: primary - phospho-p38 MAPK (Thr180/Tyr182) antibody (Cell Signalling), 1:1000 in 5% BSA TBST, over night incubation at 4°C; secondary - anti-rabbit antibody HRP-linked IgG (Cell Signalling), 1:2000 in 5% milk TBST, for 1 h at room temperature. Membranes were developed with Lumi Light Western Blotting Substrate (Roche), scanned using a Fuji Film LAS-1000 CCD camera with Image Reader LAS-1000 Pro V2.6 software and quantified using Multi Gauge 3.0 software.

1 ## Data sets

data set 1		
NaCl[M]	**Vol [%]**	**Sd**
-0.16	103.00	NA
-0.11	101.00	NA
-0.10	102.00	NA
0.00	100.00	4.00
0.02	101.00	NA
0.05	102.00	3.00
0.10	98.00	3.00
0.15	89.00	4.00
0.20	84.00	7.00
0.25	78.00	NA
0.30	79.00	4.00
0.40	74.00	11.00
0.50	63.00	NA
0.60	68.00	7.00
0.70	60.00	NA
0.80	63.00	7.00
1.00	61.00	3.00
1.50	54.00	NA

data set 2		
NaCl[M]	**Vol [%]**	**sd**
0.05	98.81	2.45
0.10	94.96	1.49
0.15	91.32	3.42
0.20	89.96	1.57
0.30	81.68	2.54
0.40	78.47	3.29
0.50	70.39	2.16
0.60	68.15	4.06
0.80	61.06	4.39
1.00	56.10	2.73
1.50	55.18	5.33

data set 3		
NaCl[M]	**Vol [%]**	**sd**
0.00	101.04	4.45
0.02	99.19	2.31
0.05	100.30	3.98
0.10	96.04	5.13
0.15	90.74	3.47
0.20	81.70	3.15
0.25	70.98	2.73
0.30	66.23	4.56
0.40	64.24	4.69
0.60	53.37	5.22
0.80	48.78	4.61
1.00	50.45	8.27
1.50	44.58	9.66

data set 4		
Glycerol [M]	**Vol [%]**	**sd**
0.00	100.00	0.00
0.14	99.00	2.50
0.56	96.50	1.71
0.99	94.14	2.01
1.12	89.83	1.51
1.12	89.22	8.52
1.27	92.24	2.47
1.36	89.25	1.31
1.46	92.99	1.73
1.68	84.94	3.84
2.32	83.00	5.00
3.47	70.64	6.01
5.20	66.00	3.00
7.50	71.32	9.40
12.88	66.50	1.50

Vol is the measured volume relative to the initial volume and sd is the standard deviation (see method section).

Results

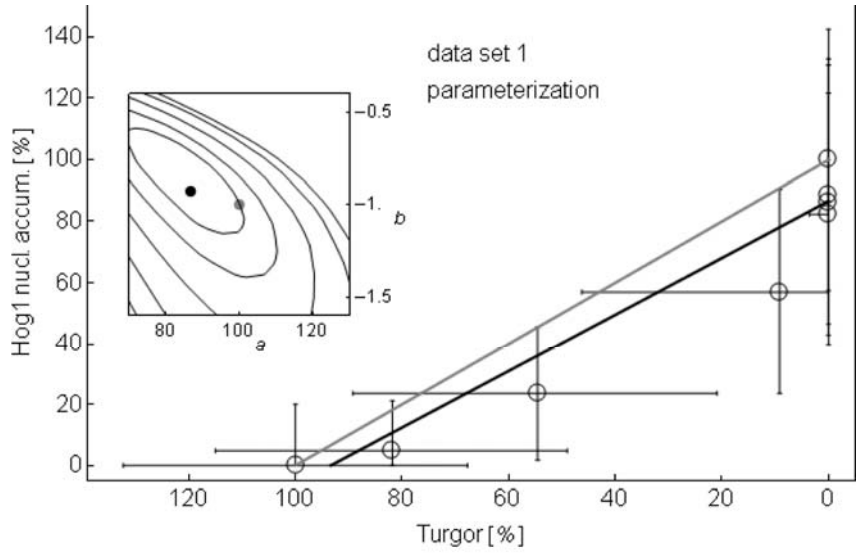
data set 1
parameterization
Hog1 nucl. accum. [%]
Turgor [%]
a
b

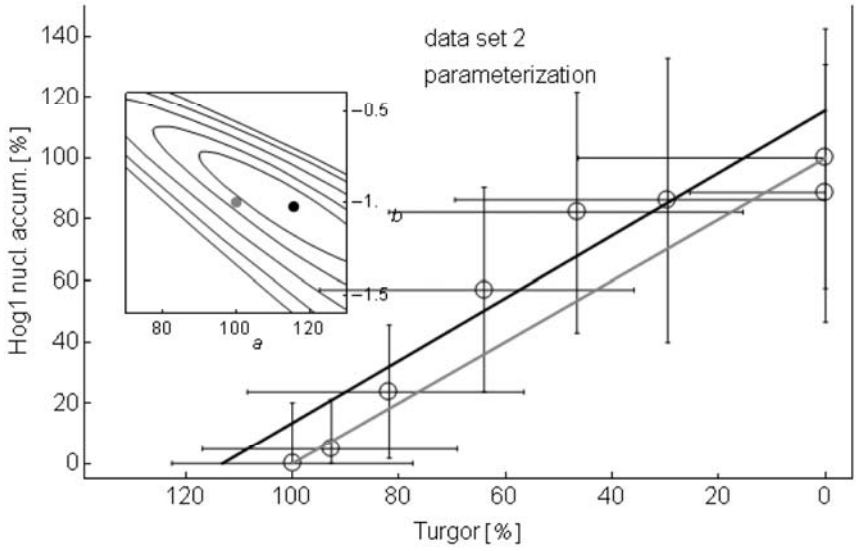
data set 2
parameterization
Hog1 nucl. accum. [%]
Turgor [%]
a
b

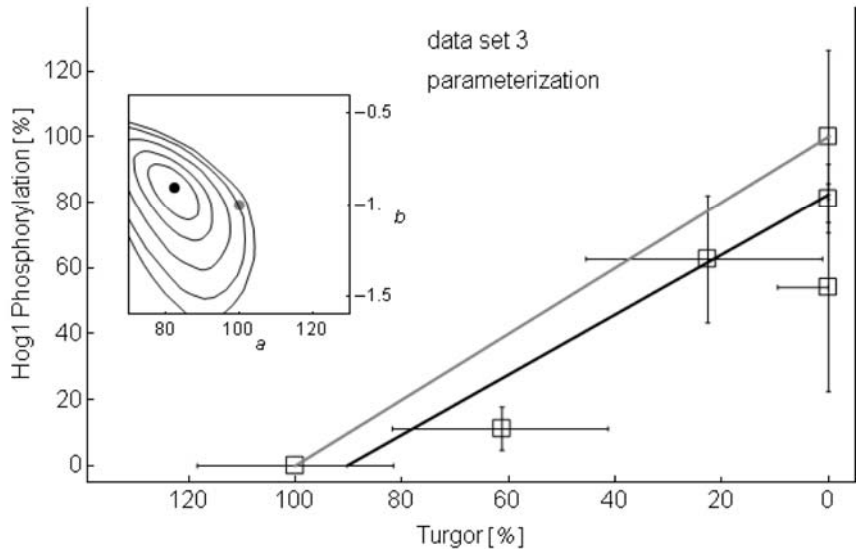
data set 3
parameterization
Hog1 Phosphorylation [%]
Turgor [%]
a
b

Figure S3: Turgor-HOG pathway activation relation. The x-axes are relative turgor [%] as predicted by the parameterized models for different shocks of NaCl (dotted line in Fig. 1). The y-axes are relative HOG pathway activation [%] according to different shocks of NaCl (Fig. 2). The black lines are a fitted linear relation ship ($y=a+bx$) by a weighted orthogonal regression. The grey lines represent the null hypothesis H_0: y=100-x, i.e. a direct 1:1 linear relation between relative loss of turgor and relative HOG pathway activation. The inset are plots of the (25%, 50%, 75%, 90%, 95%)-confidence regions of the respective estimated parameter pair (a,b) of $a+bx$ with the outermost line being the 95% confidence region. The black points correspond to the black lines in the plots, the gray points correspond to the grey lines. The confidence regions are obtained by a Monte-Carlo analysis with 1000 runs.

References

S1. Morris GJ, Winters L, Coulson GE, Clarke KJ (1986) Effect of osmotic stress on the on the ultrastructure and viability of the yeast *Saccharomyces cerevisiae*. Journal of General Microbiology 132: 2023-2034.

S2. Arnold WN, Lacy JS (1977) Permeability of cell-envelope and osmotic behavior in *Saccharomyces cerevisiae*. Journal of Bacteriology 131: 564-571.

S3. Niedermeyer W, Parish GR, Moor H (1977) Reaction of yeast cells to glycerol treatment - alterations to membrane structure and glycerol uptake. Protoplasma 92: 177-193.

S4. Slaninova I, Sestak S, Svoboda A, Farkas V (2000) Cell wall and cytoskeleton reorganization as the response to hyperosmotic shock in Saccharomyces cerevisiae. Archives of Microbiology 173: 245-252.

S5. Griffin DM (1981) Water and Microbial Stress. Adv Microb Ecol 5: 91-136.

S6. Noble PS (1969) The Boyle-Van't Hoff Relation. Journal of Theoretical Biology 23: 375-379.

S7. Kedem O, Katchalsky A (1958) Thermodynamic analysis of the permeability of biological membranes to non-electrolytes. Biochem Biophys Acta 27: 229-246.

S8. Kedem O, Katchalsky A (1961) Physical interpretation of phenomenological coefficients of membrane permeability. Journal of General Physiology 45: 143-&.

S9. Schaber J, Klipp E (2008) Short-term volume and turgor regulation in yeast. Essays Biochem 45: 147-160.

S10. Kleinhans FW (1998) Membrane permeability modeling: Kedem-Katchalsky vs a two-parameter formalism. Cryobiology 37: 271-289.

S11. Marechal PA, deMaranon IM, Molin P, Gervais P (1995) Yeast cell responses to water potential variations. International Journal Of Food Microbiology 28: 277-287.

S12. Gervais P, Molin P, Marechal PA, Herail-Foussereau C (1996) Thermodynamics of yeast cell osmoregulation: passive mechanisms. J Biol Phys 22: 73-86.

S13. Hohmann S (2002) Osmotic stress signaling and osmoadaptation in yeasts. Microbiol Mol Biol Rev 66: 300-372.

S14. Klipp E, Nordlander B, Kruger R, Gennemark P, Hohmann S (2005) Integrative model of the response of yeast to osmotic shock. Nat Biotechnol 23: 975-982.

S15. Soveral G, Madeira A, Loureiro-Dias MC, Moura TF (2007) Water transport in intact yeast cells as assessed by fluorescence self-quenching. Appl Environ Microbiol 73: 2341-2343.

S16. Eriksson E, Enger J, Nordlander B, Erjavec N, Ramser K, et al. (2007) A microfluidic system in combination with optical tweezers for analyzing rapid and reversible cytological alterations in single cells upon environmental changes. Lab Chip 7: 71-76.

S17. Gennemark P, Nordlander B, Hohmann S, Wedelin D (2006) A simple mathematical model of adaptation to high osmolarity in yeast. In Silico Biol 6: 193-214.

S18. Eriksson E, Sott K, Lundqvist F, Sveningsson M, Scrimgeour J, et al. A microfluidic device for reversible environmental changes around single cells using optical tweezers for cell selection and positioning. Lab Chip 10: 617-625.

S19. Chernomoretz A, Bush A, Yu R, Gordon A, Colman-Lerner A (2008) Using Cell-ID 1.4 with R for microscope-based cytometry. Curr Protoc Mol Biol Chapter 14: Unit 14 18.
S20. Gordon A, Colman-Lerner A, Chin TE, Benjamin KR, Yu RC, et al. (2007) Single-cell quantification of molecules and rates using open-source microscope-based cytometry. Nat Methods 4: 175-181.
S21. Thomas BJ, Rothstein RJ (1989) Elevated recombination rates in transcriptionally active DNA. Cell 56: 619-630.